Journal of Catalysis **209,** 245–255 (2002)
doi:10.1006/jcat.2002.3633

Characterization of *ex Situ* Presulfided Ni/Al_2O_3 Catalysts for Pyrolysis Gasoline Hydrogenation

Bram W. Hoffer,*,[1] François Devred,† Patricia J. Kooyman,† A. Dick van Langeveld,‡ Raimond L. C. Bonné,§ Clive Griffiths,‖ C. Martin Lok,‖ and Jacob A. Moulijn*

*Reactor & Catalysis Engineering, Delft University of Technology, Julianalaan 136, 2628 BL Delft, The Netherlands; †National Centre for High Resolution Electron Microscopy, Delft University of Technology, Rotterdamseweg 137, 2628 AL Delft, The Netherlands; ‡Charged Particle Optics Group, Delft University of Technology, Lorentzweg 1, 2628 CJ Delft, The Netherlands; §Synetix, Steintor 9, D-46446 Emmerich, Germany; and ‖Synetix, P.O. Box 1, Belasis Avenue, Billingham, Cleveland TS 23 1LB, United Kingdom

Received February 7, 2002; revised March 28, 2002; accepted March 28, 2002

Partially sulfided oxidic as well as reduced and passivated Al_2O_3-supported nickel catalysts for pyrolysis gasoline hydrogenation were successfully prepared by *ex situ* presulfidation with di-*tert*-butyl polysulfide followed by *in situ* reduction. The catalysts were characterized by temperature-programmed reduction (TPR), temperature-programmed desorption (TPD), high-resolution transmission electron microscopy (HRTEM), and Raman spectroscopy. The Ni particles in the catalysts are covered with a limited amount of sulfur, which depends on the sulfur loading. Complete saturation of the Ni monolayer has been reached between 1.0 and 2.0 wt% S, corresponding to a S/Ni_{surf} atomic ratio of 0.2–0.5. From TPD and extraction experiments it was inferred that the excess of sulfide, exceeding monolayer coverage, is weakly bound to the support. The high dispersion of the catalysts was maintained during sulfidation. TPR showed that the presulfided oxidic catalysts can be activated (by reduction) at lower temperatures ($\Delta T = 150$ K) than the nonsulfided oxidic catalyst. This eliminates the intermediate reduction and passivation procedure, resulting in more efficient catalyst activation procedures.

Key Words: **Ni; alumina; TPR; TPD; HRTEM; Raman spectroscopy; presulfiding; sulfidation; activation; pygas; hydrogenation.**

INTRODUCTION

Alumina-supported nickel catalysts are used in petrochemical and refining processes, for example in pyrolysis gasoline (pygas) hydrogenation. A highly selective Ni hydrogenation catalyst for the conversion of di-olefinic hydrocarbons into mono-olefinic hydrocarbons can be obtained by the partial sulfidation of the nickel (1–4). This partial sulfidation step is crucial to obtain a catalyst, removing gum and resin precursors in pygas (5), while maintaining a high octane number. In these partially sulfided catalysts, the surface of the Ni particles is covered with a small amount of sulfur, leading to the desired selectivity. The local geometry of S on three low-Miller-index faces in the outer layer of partial sulfided nickel has been studied extensively with polarization-dependent EXAFS (6–9). Dependent on the low-index surfaces, different high symmetry adsorption sites for sulfur can be distinguished:

—three-fold hollow sites on Ni(110)$c(2 \times 2)$-S (6);
—three-fold hollow sites on Ni(111)$p(2 \times 2)$-S (7); and
—four-fold hollow sites on Ni(100)$c(2 \times 2)$-S (8).

The monolayer of sulfide, which does not vary significantly for different surface orientations, corresponds to ca. 0.5 sulfur atom per nickel atom for the (100) surface $c(2 \times 2)$ and to 0.4 on the dense (111) surface.

For the sulfidation of the oxidic catalyst precursors, three different procedures can be applied (10):

1. reduction of the oxidic catalyst followed by sulfidation of the reduced catalyst;
2. simultaneous reduction and sulfidation of the oxidic catalyst;
3. sulfiding of the catalyst followed by reduction.

The first two routines are the most commonly applied, where H_2 usually is applied for the *in situ* reduction. In the first option the reduced catalyst is sulfided by spiking the feed with reactive sulfur-containing molecules. For the second option a mixture of hydrogen and reactive sulfur-containing molecules is applied. These sulfur-containing compounds are malodorous, toxic, and volatile; moreover, this *in situ* sulfidation is a relatively difficult and time-consuming procedure. The conventional presulfiding procedure can only be carried out at those conditions where sulfiding results in one or more surface sulfide layers constituting a diffusion barrier either for sulfur diffusion into the bulk of nickel crystallites or for diffusion of nickel ions into the surface layers. Thermodynamic calculations show that at high sulfur concentrations and low temperatures bulk nickel sulfide will be formed, thus resulting in oversulfiding and, hence, loss of activity (1, 11, 12).

[1] To whom correspondence should be addressed. Fax: +31 (0)152785006. E-mail: b.w.hoffer@tnw.tudelft.nl.

0021-9517/02 $35.00

A more elegant way would be to employ *ex situ* presulfided catalysts (13–15). In this process the oxidic nickel precursor is presulfided off-site into a non toxic, stable, odorless catalyst. This catalyst can be activated *in situ* during start-up under hydrogen in the feedstock. No additional sulfur is required in this process. In hydrotreating processes in oil refineries such a procedure is now state of the art.

The objective of the present work is to establish a relationship between the preparation and resulting properties of a range of *ex situ* presulfided Ni/Al_2O_3 catalysts with varying sulfur loading. The current paper describes the characterization of the catalysts by temperature-programmed decomposition (TPD), temperature-programmed reduction (TPR) in a flow reactor, quasi *in situ* high-resolution transmission electron microscopy (HRTEM), and TPR monitored by *in situ* laser Raman spectroscopy (LRS). The incentive of the characterization is to acquire insight into the activation process of presulfided catalysts in a hydrogen atmosphere at elevated temperatures and to develop a model, that describes the mechanism of sulfidation and activation in the preparation procedure of *ex situ* presulfided Ni/Al_2O_3 catalysts.

METHODS

Ex Situ Presulfiding

In this study two commercially available catalysts (HTC200, Synetix) were used as starting material for the preparation of presulfided catalysts. Synetix has prepared both catalysts by pore volume impregnation of a transition alumina support, followed by drying and calcination. The second catalyst, referred to as R-P, has been made from the first, oxidic, catalyst by reduction under hydrogen flow and subsequent passivation in a nitrogen-diluted flow of oxygen. Both starting materials have recently been characterized extensively (1, 16). The nickel content (11.9 wt%) was determined by ICP-AAS.

The *ex situ* presulfided catalysts were obtained by impregnation of the Ni/Al_2O_3 catalysts (oxidic and the R-P) with a solution of an organic polysulfide in an excess of *n*-heptane in a rotary evaporator. The presulfiding agent used in this procedure was a di-*tert*-butyl polysulfide (i.e., C_4H_9-S_x–C_4H_9, where S_x represents a linear polysulfide chain with an average length of 4.2 S atoms). The concentration of the impregnation solution was varied to obtain a range of presulfided catalysts with sulfur loading around the point of monolayer sulfidation. The *n*-heptane was removed and after drying in static air at 425 K the presulfided catalyst was stored under air.

The sulfur loading was determined with a Namas accredited LECO analyzer. Tables 1 and 2 summarize the characteristics of the presulfided oxidic (O-S) and presulfided reduced and passivated (R-P-S) catalysts. The nickel surface area of the reduced, presulfided catalysts was evaluated from H_2 chemisorption by extrapolation of the total amount of both reversible and irreversible adsorbed hydrogen to zero pressure. The nickel surface area was calculated under the assumptions that one Ni surface atom chemisorbs one hydrogen atom and one Ni atom occupies 0.0645 nm^2 (17). To establish homogeneous sampling for all experiments and to avoid mass- and heat-transfer limitations in the temperature-programmed reactions, the catalyst extrudates were crushed and sieved, and the particle size fraction between 63 and 180 μm was used.

TABLE 1

Codes and Characteristics of the Oxidic Ni Catalysts

Catalyst	Code	S[a] (wt%)	S_{Ni}[b] ($m^2 \cdot g_{Ni}^{-1}$)
Presulfided support	Al-S	1.2	0.0
Oxidic	O	0.0	170.0
Presulfided oxidic	O-S(1)	0.2	100.0
	O-S(2)	0.6	14.3
	$O\text{-}S(2)_{EXTR}$[c]	0.8	—
	O-S(3)	1.0	8.4
	O-S(4)	2.0	1.1
	O-S(5)	4.2	B.D.L.[d]
	$O\text{-}S(5)_{EXTR}$	2.7	B.D.L.[d]

[a] Sulfur concentration.
[b] Ni surface area determined by H_2 chemisorption.
[c] Catalyst after extraction in toluene.
[d] B.D.L.: below detection limit.

TPD and TPR

The decomposition of the polysulfides on the presulfided catalysts was studied by TPD in an atmospheric plug-flow reactor. The weight of the catalyst sample was in the range of 100 to 150 mg. After being introduced into the reactor, the catalyst was purged with Ar for 0.5 h. After stabilization of the system, the sample was heated in an Ar flow

TABLE 2

Codes and Characteristics of the R-P Ni Catalysts

Catalyst	Code	S[a] (wt%)	S_{Ni}[b] ($m^2 \cdot g_{Ni}^{-1}$)
Reduced and passivated	R-P	0.0	137.0
Blank R-P	R-P-B	0.0	—
Presulfided R-P	R-P-S(1)	0.3	35.3
	R-P-S(2)	0.8	1.7
	R-P-S(3)	1.0	6.0
	R-P-S(4)	2.0	—
	R-P-S(5)	4.2	B.D.L.[c]

[a] Sulfur concentration.
[b] Ni surface area determined by H_2 chemisorption.
[c] B.D.L.: below detection limit.

of 26 μmol s^{-1} according to a linear temperature program with a heating rate of 0.167 K s^{-1}. In the reactor effluent the H_2S concentration was monitored with an UV spectrometer tuned to 205 nm. The presence of hydrocarbons in the effluent was monitored with a flame ionization detector (FID). The reduction behavior of the presulfided catalysts was also studied in this reactor system. A gas mixture consisting of 8 μmol s^{-1} H_2 and 19 μmol s^{-1} Ar was employed. The hydrogen concentration was monitored with a thermal conductivity detector (TCD). A detailed description of the TPR/TPD apparatus has been given by Arnoldy *et al.* (18).

Toluene Extraction Experiments

To establish the degree of fixation of the sulfiding agent, two catalyst samples were extracted in boiling toluene. The experiments were carried out with the catalyst extrudates in a Soxhlet extraction setup for 7 h. After being extracted the catalysts were dried in air and a TPR run was performed with both the freshly presulfided catalysts and the extracted presulfided catalysts. Table 1 summarizes some characteristic properties of the extracted samples ($O\text{-}S(2)_{EXTR}$ and $O\text{-}S(5)_{EXTR}$).

In Situ Laser Raman Spectroscopy in TPR

The experiments were performed with a Renishaw Ramascope system 2000 coupled with a Leica microscope. The excitation source is a 514-nm, 20-mW Ar^+ laser with an excitation power of 2 mW. Scattered Raman light is collected by the objective, filtered for Rayleigh scattering, and coupled to the spectrograph. The spectrograph with holographic optics dispersed the light over the CCD detector, which was read via a PC to obtain the Raman spectrum with a resolution of 2 cm^{-1}. The temperature-programmed reductions were carried out in a high-temperature resistant cell (Linkam TS1500) with a hydrogen flow of 10 μmol s^{-1}. Optionally, mild oxidation in a N_2/air flow at room temperature was applied after reduction.

Quasi in Situ HRTEM

Quasi *in situ* HRTEM was performed using a Philips CM30T electron microscope equipped with a LaB_6 electron source operated at 300 kV. Samples were applied on a microgrid carbon polymer supported on a copper grid by placing a few droplets of a suspension of ground sample in *n*-hexane on the grid, followed by drying at ambient conditions, all in an Ar glovebox. The catalysts were investigated as such and after reduction in hydrogen at 673 K for 1 h. Samples were transferred to the microscope in a special vacuum-transfer sample holder under exclusion of air (19). The distribution of the crystallite sizes was determined by counting at least 100 Ni crystallites per sample from different HRTEM pictures taken at different catalyst grains.

RESULTS

TPD

The TPD-FID profiles of the presulfided oxidic nickel catalysts are collected in Fig. 1a. Up to a sulfur loading of 1.0 wt% (the O-S(3) sample) the patterns of the catalysts are similar. For these catalysts three peaks can be distinguished in the FID signals (i.e., hydrocarbon detection). At about 455 K a small peak can be observed, while two larger peaks can be seen at about 530 and 630 K. The intensity of the peaks increases with increasing sulfur loading. At higher sulfur loading the catalysts show a totally different behavior. One large, relatively sharp peak appears at 495 K, followed by a small peak at 595 K. Note that the signals of the O-S(4) and O-S(5) catalysts are normalized to 10 mg of catalyst sample, whereas those of all other catalysts are normalized to 100 mg of catalyst. The profile of the presulfided Ni-free alumina carrier (Al-S) shows a contribution at 495 K, comparable to the high S loaded catalysts. In Fig. 1b the TPD profiles of the presulfided R-P catalysts are collected, and they follow the same trend as the oxidic counterparts. However, the peak at 455 K for the R-P-S catalysts is smaller and very small for the R-P-S(2) compared to the presulfided oxidic catalysts.

In the UV pattern, representing the presence of H_2S in the reactor effluent, no signals were detected.

TPR

The TPR profiles of the presulfided oxidic catalysts are presented in Fig. 2a. The oxidic precursor (O) shows a broad hydrogen consumption signal between 500 and 900 K. An additional, sharp, relatively small peak at 623 K can be observed. After introduction of sulfur, the peak centered at 623 K disappears and a new peak appears at about 575 K. This new peak becomes larger with increasing sulfur loading, while the broad peak disappears. Hence, two regions can be distinguished: a contribution peaking at around 575 K and a broad signal peaking at around 700 K. The integrated hydrogen consumption of the two regions has been quantified and normalized to the nickel content. The data are summarized in Table 3. The high S loaded O-S(4) and O-S(5) catalysts show an additional small peak at 490 K, while the contribution in the high-temperature region has disappeared.

The hydrocarbon production due to decomposition of the polysulfides during TPR was also monitored and the resulting patterns are collected in Fig. 2b. The patterns look similar to the TPD profiles in Fig. 1a. However, it should be noted that an additional contribution can be observed at around 600 K for the low S loaded catalysts and the bare alumina carrier.

Figure 3 shows the TPR profiles of the presulfided R-P catalysts. The influence of the polysulfide on the dispersion

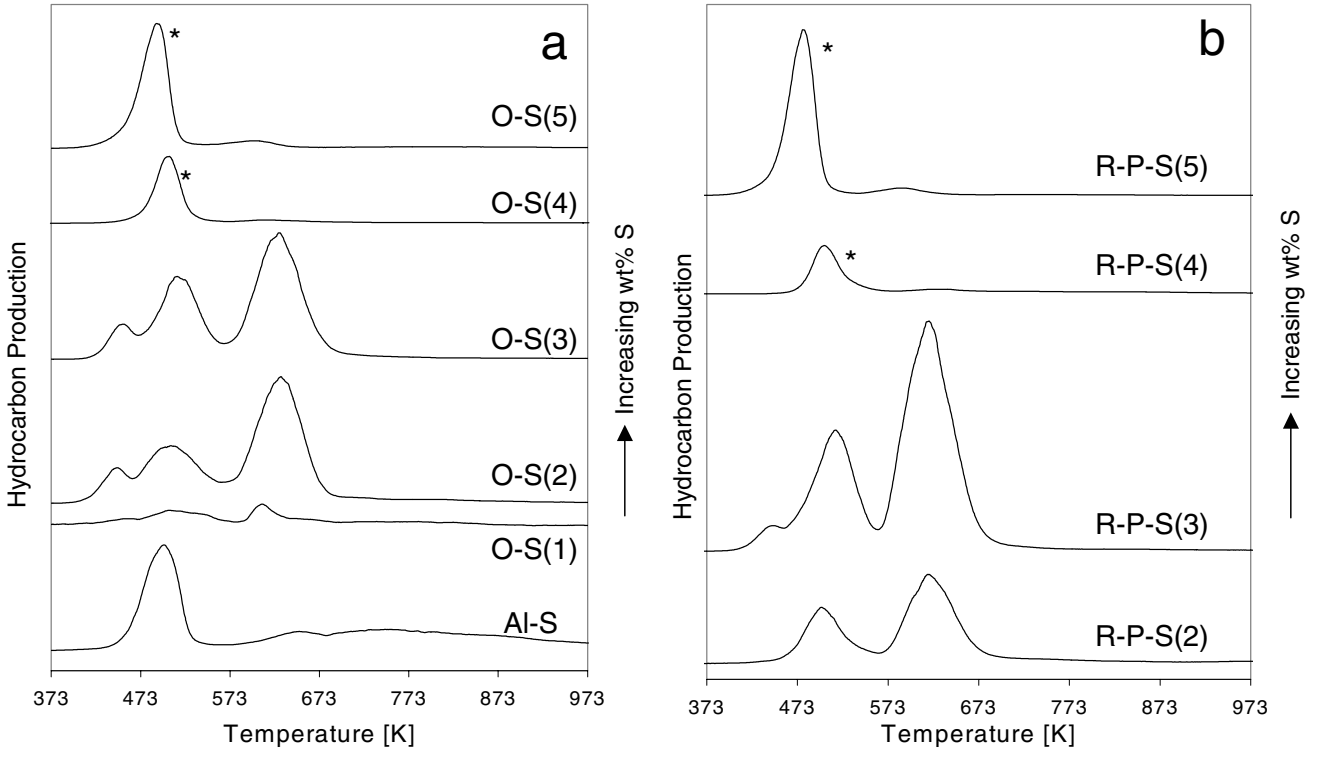

FIG. 1. TPD-FID profiles of the presulfided oxidic nickel catalysts (a) and presulfided R-P nickel catalysts (b). The profiles are normalized to 100 mg of catalyst, except for the high S loaded catalysts (indicated by ∗), which are normalized to 10 mg of catalyst. For codes see Tables 1 and 2.

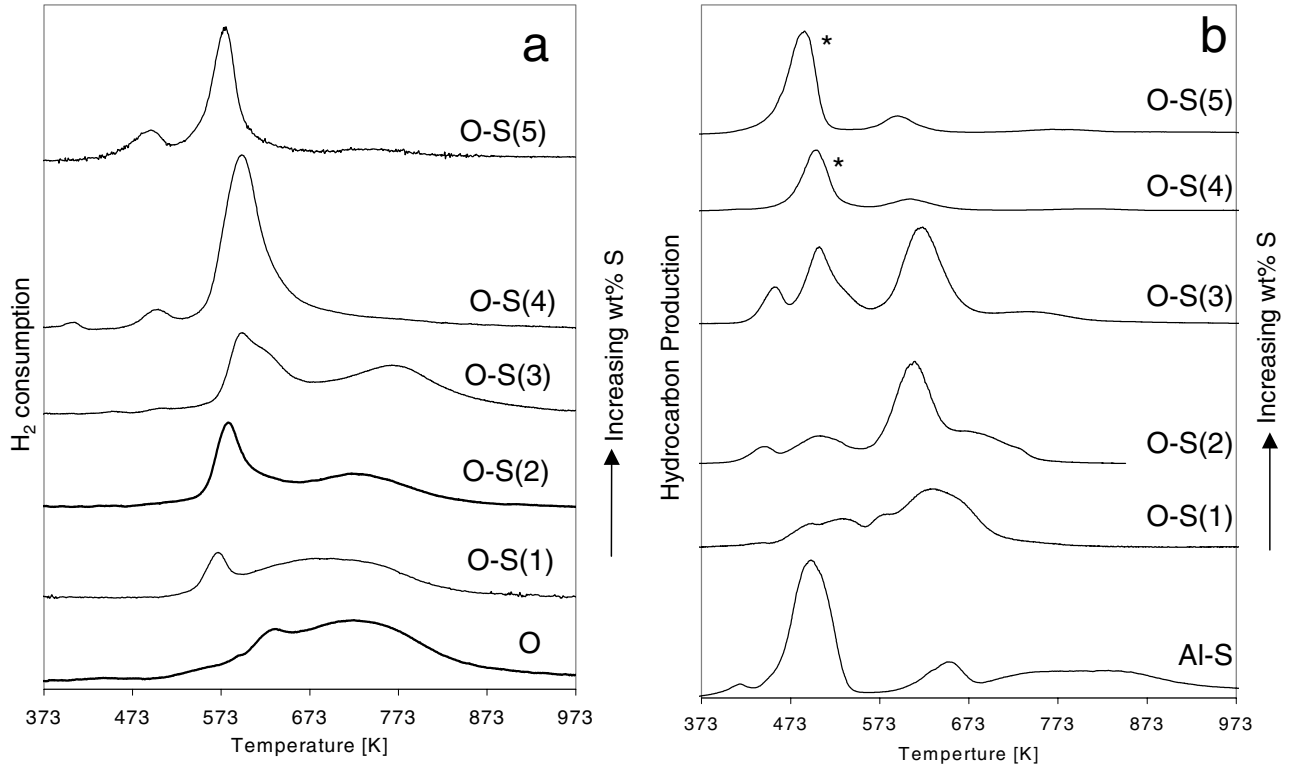

FIG. 2. TPR profiles of the presulfided oxidic catalysts. (a) Hydrogen consumption (TCD) and (b) hydrocarbon production (FID). The profiles are normalized to 100 mg of catalyst, except for FID signals of the high S loaded catalysts (indicated by ∗), which are normalized to 10 mg of catalyst. For codes see Table 1.

TABLE 3

Quantified TPR Results of Oxidic Catalysts

Catalyst	H_2/Ni (mol mol^{-1}) peak at 575 K	H_2/Ni (mol mol^{-1}) peak at 700 K	H_2/Ni (mol mol^{-1}) total
O	0.0	1.4	1.4
O-S(1)	0.1	0.9	1.0
O-S(2)	0.3	0.8	1.2
O-S(3)	0.3	0.9	1.2
O-S(4)	1.2	0.0	1.2
O-S(5)	0.7	0.0	0.7

during the presulfiding was checked using an identical impregnation treatment as for the other presulfided catalysts, but without the polysulfide in the solvent. The TPR pattern of this catalyst sample (R-P-B) shows behavior similar to that of the original untreated RP catalyst (R-P). For all samples, the main hydrogen consumption signal occurs in a well-defined peak with a maximum at around 573 K. This peak has a shoulder at the high-temperature side after presulfidation, which is more developed at higher S loading. Furthermore, an additional hydrogen consumption is observed, peaking at higher temperatures (700 K) for the catalysts with no or low S loading than for the catalyst with higher loading. The R-P-S(5) catalyst system shows an additional peak at relatively low temperature (500 K). As was also the case for the oxidic catalysts, the hydrocarbon production behavior in TPR corresponds nicely to the TPD results.

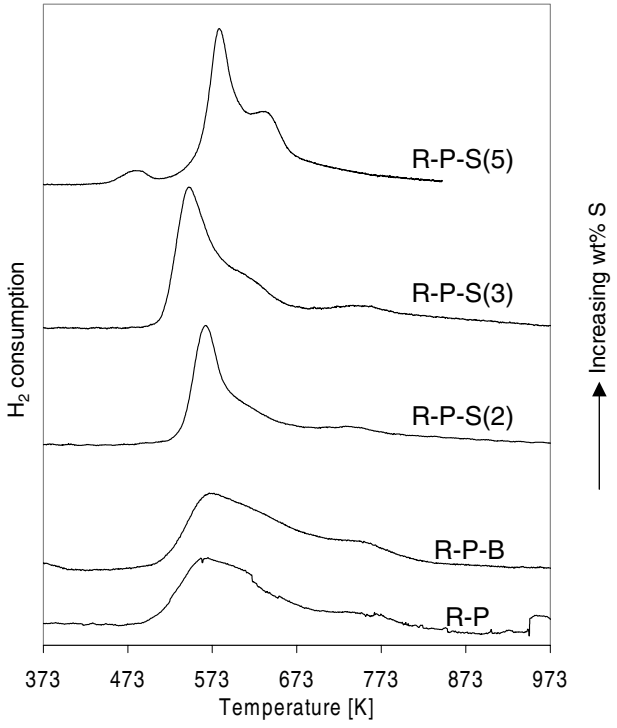

FIG. 3. TPR profiles of the presulfided R-P nickel catalysts: hydrogen consumption (TCD). The profiles are normalized to 100 mg of catalyst. For codes see Table 2.

Toluene Extraction Experiments

The results of the toluene extraction experiments have been evaluated by means of TPR. Figure 4 shows the FID profiles (representing the release of hydrocarbons) of the O-S(5) catalyst, before and after extraction. For the high loaded O-S(5) catalyst the signal of the peak at 495 K has been reduced after toluene extraction to about 80% of its original height, whereas the area of the contribution peaking at about 595 K remains more or less constant. The desorption of hydrocarbons under reducing conditions is less affected by the toluene extraction for the low sulfur loaded O-S(2) catalyst. The contribution at low temperature (455 K) has disappeared in the FID pattern after the toluene treatment. Again, the desorption contribution at 595 K has not changed. Table 1 also shows that the O-S(5) catalyst loses much of its sulfur whereas the sulfur concentration of the O-S(2) sample remains constant within the limits of experimental accuracy.

HRTEM

Figure 5a shows the distribution of crystallite sizes on the high S loaded oxidic Ni catalyst. The particle sizes vary from 3 to 8 nm. Particles on the nonsulfided and low S loaded oxidic catalysts could not be detected. Figure 5b shows the distribution of crystallite sizes of the reduced low S loaded and the high S loaded catalysts. It can be seen that upon reduction the high S loaded catalyst shows Ni crystallites with sizes in the same range as before reduction. The reduced O-S(2) sample has crystallites of about 3 nm, whereas the reduced O-S(5) sample consists of particles with a size of about 4 nm.

Figure 5c shows that the low S loaded R-P catalyst has smaller crystallites (2–5 nm) compared to the high S loaded sample (2–6 nm). Upon reduction the particle size of both samples increases.

In Situ LRS

Figure 6 shows the Raman spectra of the presulfided oxidic catalysts at room temperature in a hydrogen atmosphere. The oxidic catalyst, O, gives bands at 554 and 1100 cm^{-1} and a broad signal at around 3600 cm^{-1}. Adding the presulfiding agent according to the given procedure leads to development of two relatively small contributions at 997 and 1044 cm^{-1} and a sharp peak at 2934 cm^{-1}. Up to 1.0 wt% S, the amount of sulfur has no effect on the Raman bands at 554 cm^{-1}. However, for the O-S(5) sample, the contribution at 554 cm^{-1} has disappeared. Moreover, the intensity of the large band at around 3600 cm^{-1}, which

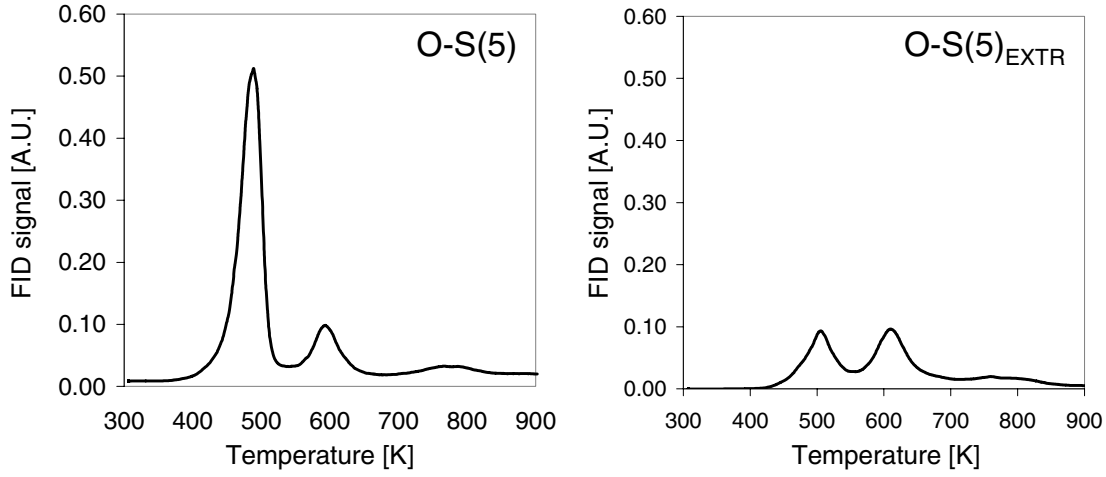

FIG. 4. Impact of toluene extraction on the TPR profiles of the O-S(5) catalyst. The signals represent the hydrocarbon decomposition (FID). (Left) TPR pattern before toluene extraction; (right) the pattern after extraction.

increases initially with increasing degree of sulfidation, has decreased dramatically. Various spectra taken at different positions in the extrudate showed that the presulfidation was uniform throughout the extrudate for all investigated catalysts.

Temperature-programmed reduction was also studied by means of LRS. As a typical result, the spectra of O-S(2) are presented in Fig. 7a. Again, the bands from the oxidic precursor can be seen at 554 and around 3600 cm^{-1}. As was already shown in Fig. 6, impregnation with the polysulfide

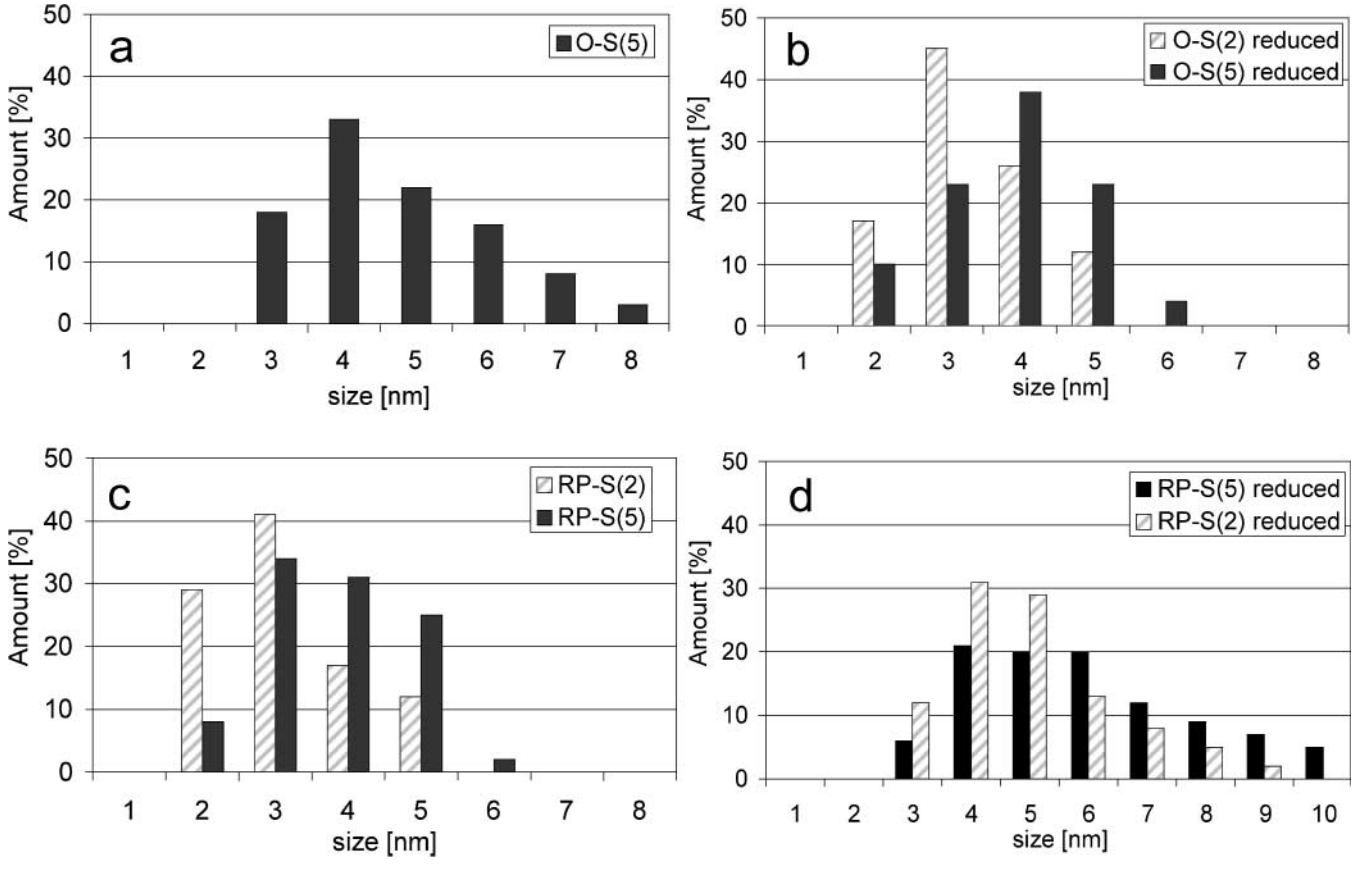

FIG. 5. Crystallite size distribution of the active phase determined with HRTEM. Presulfided oxidic catalysts before (a) and after reduction (b). Presulfided R-P catalysts before (c) and after reduction (d).

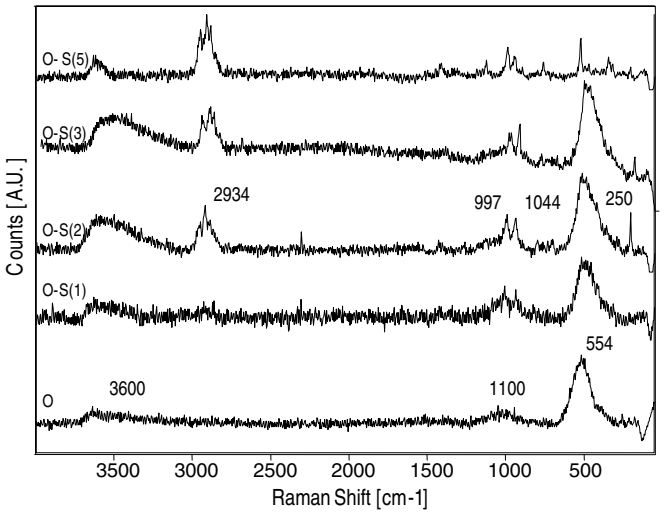

FIG. 6. Raman spectra of the presulfided oxidic catalysts for various S loading.

leads to an additional sharp peak at 2934 cm^{-1}, some small peaks in the 900–1100 cm^{-1} region, and one very sharp peak at 250 cm^{-1}. Between 330 and 385 K the bands change dramatically. The contribution at 554 cm^{-1} has completely disappeared, as is the case in reduction of the oxidic precursor, and a large broad band evolves in the 1300–1700 cm^{-1} region. However, this broad band declines with increasing temperature. At 435 K, a sharp peak can be detected at 320 cm^{-1}. The small peaks in the 900–1100 cm^{-1} region slowly disappear with increasing temperature and are almost completely gone at 535 K. After the *in situ* cell has been cooled and the reduced presulfided catalyst has been mildly oxidized in an air/nitrogen stream, the band at 554 cm^{-1} appears again. The same treatment did not result in a reappearance of this contribution for the high S loaded O-S(5) catalyst (Fig. 7b). However, the intermediate species with contributions between 1300–1700 cm^{-1} are also observed.

DISCUSSION

Decomposition of the Polysulfides

Comparing the TPD patterns and the hydrocarbon production patterns from the TPR experiments of both oxidic and R-P catalysts suggests that the polysulfides are decomposed due to the increase in temperature and that the decomposition does not involve a reaction with hydrogen. However, the additional contribution at around 600 K as observed in the hydrocarbon production for both the bare alumina carrier and the catalysts indicates that the last stage of decomposition is slightly affected by the presence of hydrogen. The decomposition of the polysulfide starts at 455 K, in good agreement with thermal decomposition (TGA) experiments with the pure presulfiding agent in hydrogen flow (20). For the low S loaded oxidic catalysts the TPD patterns show three peaks, indicating that the polysulfide decomposes in three steps (Fig. 1a). As for the catalysts with higher sulfur loading, a very large peak is observed at 495 K with a much smaller peak at 595 K. Since this large peak at 495 K can also be seen in the TPD profile of the

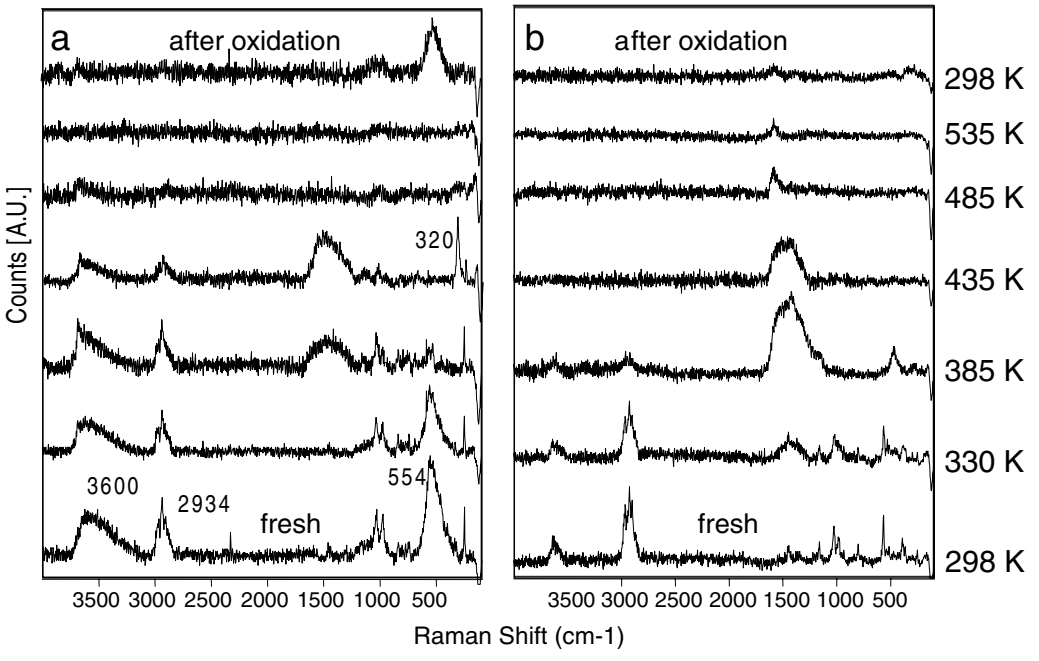

FIG. 7. Raman spectra in TPR mode of O-S(2) (a) and O-S(5) (b) catalysts with increasing temperature. The upper spectrum of both catalysts has been recorded after passivation of the catalyst at room temperature under a flow of air in N_2.

bare alumina carrier and the peak at 595 K can hardly be seen, it is suggested that the latter can be attributed to a species more strongly bound to the surface. The first peak can be attributed to a weakly adsorbed species: excess of sulfiding agent is present on the high S loaded catalysts. This is in line with the toluene extraction (Fig. 4). The intensity of the peak at 495 K, representing the desorption of hydrocarbons for the high S loaded catalyst, i.e., O-S(5), has been reduced to about 20% of its original value after extraction in toluene. In contrast, the peak at 595 K has a comparable intensity before and after the extraction procedure. Also, the total S analysis (see Table 1) reveals that a significant part of the sulfur (35 wt%) has been removed by the extraction step. This is a clear indication that a large amount of the polysulfides is weakly bound in this high loaded catalyst. For the low loaded O-S(2) catalyst, toluene treatment did not result in large differences in either the TPR pattern or the sulfur content of the catalyst, indicating that the polysulfides are chemically bound to the catalyst.

Nature of the Active Phase

TPR of the sulfur free oxidic and R-P Ni/Al_2O_3 catalysts has been extensively discussed in a recent paper (1). The oxidic catalyst has an excess of oxygen. It was furthermore concluded that no nickel aluminates were present and upon reduction and passivation the reducibility increases due to formation of a metallic kernel and a nickel oxide skin. Introduction of polysulfide in the oxidic catalyst has a dramatic effect on the reducibility of the resulting catalysts. After sulfidation two peaks at different temperature regions can be observed. Table 3 gives a quantification of the two regions observed in TPR. It can be seen that the excess of oxygen has disappeared during the presulfiding procedure. Since no formation of H_2S was observed during reduction and desorption of the hydrocarbons does not involve a reaction with hydrogen, the consumption of hydrogen must be attributed to a reaction with an oxygen species. Therefore, it can be concluded that two kinds of oxygen species are present on the catalyst surface after impregnation of the polysulfides. At high temperature NiO reduces to metallic Ni, whereas the contribution at low temperature must be reduction of an oxy-sulfidic species which will lead to the desired Ni sulfide phase and loss of the hydrocarbon tails. Above 1 wt% S all NiO has reacted with the polysulfides. The following equations give the origin of the active species:

Impregnation:

$$Ni{-}O + C_xH_yS_z \rightarrow Ni{-}O{-}S_z{-}C_xH_y \qquad [1]$$

Reduction at elevated temperature:

$$Ni{-}O{-}S_z{-}C_xH_y + H_2 \rightarrow Ni{-}S_z + H_2O + C_xH_y \qquad [2]$$

$$Ni{-}O + H_2 \rightarrow Ni^0 + H_2O. \qquad [3]$$

During impregnation, the polysulfides react with NiO according to the sulfiding mechanism proposed by Arnoldy *et al.* (21) and Mangnus *et al.* (11), where the polysulfides adsorb and form Ni–S bands. Upon reduction, formation of Ni sulfide species takes place.

Remarkably, in the TPR patterns of the presulfided oxidic catalysts, the major hydrogen consumption occurs at temperatures which are very similar to those of their R-P counterparts. Hence, the R-P pretreatment is not useful for the presulfided catalysts. *In situ* LRS experiments with the sulfided catalysts support the conclusion that above 1.0 wt% S the NiO is totally covered with sulfur. The contribution at 554 cm^{-1}, representing Ni–O vibrations of supported NiO (22–25), has disappeared in the O-S(5) sample (Fig. 6). The existence of this contribution for the low S loaded catalysts, however, indicates that during the presulfiding procedure some NiO remains available at the catalyst surface, as was also concluded from TPR. CH_2-stretch vibrations at 2934 cm^{-1} and C–C stretching modes in the 900–1100 cm^{-1} region prove that polysulfides are also present on the samples. The small peak at 250 cm^{-1} can be attributed to a NiS species. Bishop and co-workers studied Raman spectra of high-purity NiS in both α and β forms and found intense vibrational frequencies at 246–238 and 174 cm^{-1} (26). The TPR of the O-S(2) catalyst sample monitored by LRS showed that the NiO is gradually reduced and has disappeared between 385 and 435 K, leading to the formation of a sharp peak at 320 cm^{-1} (Fig. 7a). Since Ni_2S_3 has never been detected so far with Raman spectroscopy and high-purity α-NiS and β-NiS have modes at 246–238 cm^{-1} (26), the contribution at 320 cm^{-1} indicates the presence of a nickel oxide species. Recently, several authors showed in Raman spectroscopy experiments with bulk nickel hydroxide that vibration of the Ni–OH lattice results in a band at 315 cm^{-1} (22, 25). Possibly some NiOH groups are formed at the catalyst surface while the catalyst is reduced in hydrogen. The appearance of a small additional contribution at around 3700 cm^{-1} supports this suggestion. The hydroxide reacts further into Ni^0 at higher temperatures, because a band is no longer observed in the low energy region. Upon mild oxidation the Ni–O band at 554 cm^{-1} reappears, indicating that the reaction is reversible. The absence of this NiO vibration after exposure of the reduced O-S(5) sample in the Raman *in situ* cell to oxygen shows that the Ni surface is less susceptible for mild oxidation than the O-S(2) catalyst, possibly because the surface is completely saturated with sulfur (Fig. 7b). At elevated temperature a broad band can be seen from 1300 to 1700 cm^{-1}, which can be attributed to formation of the oxy-sulfidic species involved in the reaction of the polysulfide chemisorbed to the NiO crystallites.

Influence of the Pretreatment on the Stability of the Ni Crystallites

The absence of H_2S production for all catalysts during the reduction indicates that the NiS_x species formed are highly stable. This is in agreement with previous work on the

NiO/Al_2O_3 system (27, 28). Scheffer *et al*. concluded that highly dispersed sulfided Ni species in the Ni/Al_2O_3 catalysts are stabilized against reduction by Ni–O–Al links (28).

The difference in results in HRTEM of the low and high S loaded presulfided oxidic catalyst is remarkable (Fig. 5). Oxidic presulfided catalysts with sulfur loading up to 1.0 wt% show occasionally relatively large crystallites of 2–3 nm, but most of the alumina surface investigated contains undetectable small crystallites (<1.0 nm), as is the case for the nonsulfided oxidic catalyst. Evidence for very small crystallites was also found in an EXAFS analysis of the oxidic nickel catalyst (16) as well as in XPS experiments described in a previous paper (1). In that paper it was also shown that Ni aluminates are not present on the catalyst. Another conclusion was that after sulfidation of the catalyst with H_2S, the crystallite size increased due to the change in chemical composition rather than by sintering effects. Applying this conclusion to our current results suggests that the larger crystallites found for the high S loaded oxidic catalysts with HRTEM are due to all the surface Ni atoms being sulfided, whereas for the low loaded catalysts the original crystallites are still present. Upon reduction it can be seen that the presence of polysulfides has an effect on the crystallite size (Fig. 5b). Reduction of the high S loaded catalyst does not influence the crystallite size, but for the low S loaded catalyst the particles have grown from 1 to 3 nm. The low S loaded presulfided R-P catalyst sample has larger crystallites than the oxidic counterpart. This is because the R-P catalyst used in the impregnation procedure already has larger Ni particles than the oxidic catalyst, essentially caused by the reduction process. Consecutive presulfiding does not change this situation. However, introducing sulfur above monolayer capacity shows enhancement in crystallite size, as was also shown for the high S loaded oxidic catalyst. Reducing both R-P samples results in formation of somewhat larger Ni particles. In summary it can be concluded that:

(i) for both oxidic and R-P presulfided catalysts a low S content has almost no influence on the dispersion of the final catalyst, whereas high S loaded catalysts have an increased particle size after presulfidation;

(ii) after reduction of the low S loaded presulfided catalysts the crystallite size has slightly increased;

(iii) the Ni particle size of presulfided and activated oxidic catalysts is smaller than the corresponding R-P catalysts, but this difference is already present in the two starting materials, e.g., before the presulfiding procedure; and

(iv) the loss of dispersion of the high S loaded catalysts is caused by the change in chemical composition rather than by sintering.

Presulfiding as a Stoichiometric Reaction

Figure 2 clearly showed that up to sulfur loading of 1.0 wt% the TPR patterns of the sulfided oxidic catalysts are similar, whereas the catalysts with a sulfur loading above 2 wt% show a completely different picture, which does not change with increasing amount of sulfur. This indicates that the saturation coverage of the active nickel sites corresponds to a S/Ni_{surf} ratio of 0.2–0.5, when assuming hemispherical particles consisting of clusters of 8 or 9 Ni atoms in diameter (16). Reported saturation stoichiometries for sulfur adsorption on supported Ni catalysts vary from 0.25 to 1.3, whereas single-crystal Ni has a saturation coverage at $S/Ni_{surf} = 0.25$–0.5 for most index planes (29). Hence, it is expected that above this saturation level of 1.0–2.0 wt% S, introducing more S does not lead to additional sulfidation. In contrast, the excess of sulfur will be physisorbed on the catalyst, as was concluded from the TPD results and the extraction experiments. In Fig. 8 the Ni surface area, determined by hydrogen chemisorption, is plotted against the sulfur loading. It can be seen that from about 1.0 wt% S almost no active Ni is left at the surface: all active sites are saturated with sulfur. The additional loss of nickel surface area due to the R-P procedure can be observed in all cases.

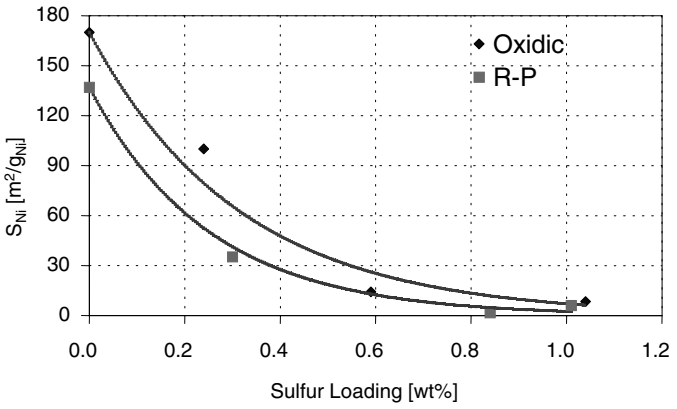

FIG. 8. The active nickel surface area as a function of sulfur loading for both oxidic as well as reduced and passivated Ni catalysts, as determined by hydrogen chemisorption.

Models

Figure 9 shows models of the presulfiding and activation of the oxidic and R-P nickel particles on the Al_2O_3 support. The oxidic catalysts consist of very small crystallites of nickel oxide and nickel hydroxide (1). Depending on the degree of sulfidation, two cases are distinguished: low sulfur loaded catalysts (<1.0 wt% S) and high loaded catalysts (>1.0 wt% S), assuming that 1.0 wt% S is the monolayer saturation. Below monolayer saturation only part of the available surface NiO has reacted with the polysulfides and some NiO is still present, as was shown with Raman spectroscopy. Above monolayer coverage all available surface nickel has reacted with polysulfides and excess of sulfide compound is adsorbed by the alumina. The size of the crystallites has

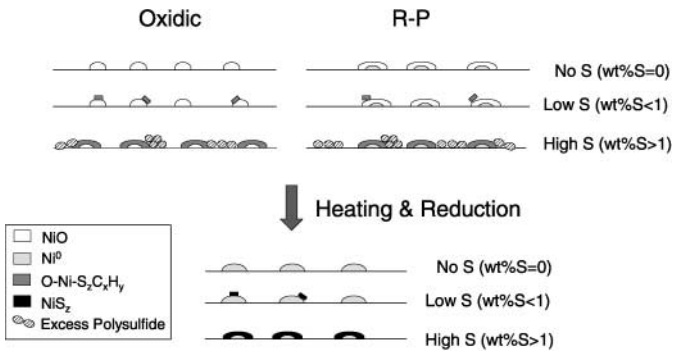

FIG. 9. A schematic representation of the presulfiding and activation process.

increased, as was observed by HRTEM. This growth can be explained by incorporation of the sulfur species into the Ni crystallite rather than by sintering of the active phase. Moreover, in previous work hydrogen chemisorption and XPS analysis showed that severe treatment with H_2S did not affect the dispersion of the catalysts under investigation (1). Reduction leads to partial sulfidation of the catalyst surface for the low loaded samples, whereas for the presulfided catalysts with an excess of sulfide, the total surface is sulfided. In the case of the R-P catalysts essentially the same result occurs as in the oxidic catalyst. However, since already a large part of the R-P catalyst crystallites consisted of metallic Ni, the impregnation procedure does not lead to species that can be reduced at significantly lower temperatures. Moreover, the loss of dispersion due to the reduction and passivation before the presulfidation step is evident, independent of the sulfur loading. Thus, reduction and passivation are not useful when the applied Ni catalysts are subsequently presulfided according to the given procedure.

CONCLUSIONS

It is possible to create partially sulfided catalysts following the preparation procedure applied. The *ex situ* presulfided catalysts are odorless and stable in air. It has been shown with temperature programmed techniques that the surface of the Ni particles in the catalysts are covered with a limited amount of sulfur, which depends on the sulfur loading. Complete saturation of the Ni monolayer is reached between 1.0 and 2.0 wt%, corresponding to a S/Ni_{surf} atomic ratio of 0.2–0.5. From TPD and toluene extraction experiments it was inferred that above monolayer coverage the excess of sulfide is weakly bound to the catalyst.

From quasi *in situ* HRTEM the Ni crystallite size of the active phase was estimated to be in the range of 2 to 3 nm after presulfidation, whereas the original oxidic catalyst comprised undetectable small crystallites. This growth in Ni particle size is relatively small and can be attributed to the change in chemical composition rather than by sintering of the active phase.

In many hydrogenation processes the use of reduced and passivated catalysts enables plant managers to use relatively low temperatures to activate the Ni catalysts. However, the reduction process is time consuming and requires very careful procedures. The use of *ex situ* presulfided oxidic catalysts can speed up the start-up of the hydrogenation process, since these catalysts can be activated at relatively low temperatures.

ACKNOWLEDGMENTS

This research has been performed under auspices of NIOK, The Netherlands Institute for Catalysis Research.

REFERENCES

1. Hoffer, B. W., Van Langeveld, A. D., Janssens, J.-P., Bonne, R. L. C., Lok, C. M., and Moulijn, J. A., *J. Catal.* **192**, 432 (2000).
2. Bourne, K. H., Holmes, P. D., and Pitkethly, *in* "Proceedings, 3rd International Congress on Catalysis, Amsterdam, 1964" (W. M. H. Sachtler, G. C. A. Schuit, and P. Zwietering, Eds.), Vol. 2, p. 1400. Wiley, New York, 1965.
3. Rostrup-Nielsen, J. R., *in* "Catalyst Deactivation 1991" (C. H. Bartholomew and J. B. Butt, Eds.), p. 85. Elsevier Science Publishers, Amsterdam, 1991.
4. Poels, E. K., Van Beek, W. P., Den Hoed, W., and Visser, C., *Fuel* **74**, 1800 (1995).
5. Petkova, N. B., *Oxid. Comm.* **22**, 186 (1999).
6. Harte, S. P., Vinton, S., Lindsay, R., Hakanson, L., Muryn, C. A., Thornton, G., Dhanak, V. R., Robinson, A. W., Binsted, N., Norman, D., and Fischer, D. A., *Surf. Sci.* **380**, L463 (1997).
7. Warburton, D. R., Wincott, P. L., Thornton, G., Quinn, F. M., and Norman, D., *Surf. Sci.* **211/212**, 71 (1989).
8. Woodhead, A. P., Harte, S. P., Haycock, S. A., Muryn, C. A., Wincott, P. L., Dhanak, V. R., and Thornton, G., *Surf. Sci.* **420**, L138 (1999).
9. Yokoyama, T., Hamamatsu, H., Kitajima, Y., Takata, Y., Yagi, S., and Ohta, T., *Surf. Sci.* **313**, 197 (1994).
10. Prada Silvy, R., Fierro, J. L. G., Grange, P., and Delmon, B., *in* "Preparation of Catalysts IV" (B. Delmon, P. Grange, P. A. Jacobs, and G. Poncelet, Eds.), p. 605. Elsevier Science Publishers, Amsterdam, 1987.
11. Mangnus, P. J., Poels, E. K., Van Langeveld, A. D., and Moulijn, J. A., *J. Catal.* **137**, 92 (1992).
12. McCarthy, J. G., and Wise, H., *J. Chem. Phys.* **72**, 6332 (1980).
13. Berrebi, G., and Roumieu, R., *Bull. Soc. Chim. Belg.* **96**, 967 (1987).
14. Labruyere, F., Dufresne, P., Lacroix, M., and Breysse, M., *Catal. Today* **43**, 111 (1998).
15. Van Gestel, J., Leglise, J., and Duchet, J.-C., *J. Catal.* **145**, 429 (1994).
16. Shido, T., Lok, C. M., and Prins, R., *Top. Catal.* **8**, 223 (1999).
17. Geus, J. W., *in* "Hydrogen Effects in Catalysis; Fundamentals and Practical Applications" (Z. Paal and P. G. Menon, Eds.), p. 85. Marcel Dekker, New York, 1988.
18. Arnoldy, P., Van den Heijkant, J. A. M., De Bok, G. D., and Moulijn, J. A., *J. Catal.* **92**, 35 (1985).
19. Zandbergen, H. W., Kooyman, P. J., and Van Langeveld, A. D., *in* "Electron Miscroscopy 1998" (H. A. Calderón Benavides and M. J. Yacamán, Eds.), Vol. 2, p. 491. Institute of Physics, Bristol, 1998.

20. SULFRZOL 54 Technical Information. Lubrizol Limited, UK, 1997.
21. Arnoldy, P., De Booys, J. L., Scheffer, B., and Moulijn, J. A., *J. Catal*. **96**, 122 (1985).
22. Bernard, M. C., Keddam, M., Takenouti, H., Bernard, P., and Senyarich, S., *J. Electrochem. Soc.* **143**, 2447 (1996).
23. Bernard, M. C., Cortes, R., Keddam, M., Takenouti, H., Bernard, P., and Senyarich, S., *J. Power Sources* **63**, 247 (1996).
24. Chan, S. S., and Wachs, I. E., *J. Catal*. **103**, 224 (1987).
25. Deabate, S., Fourgeot, F., and Henn, F., *J. Power Sources* **87**, 125 (2000).
26. Bishop, D. W., Thomas, P. S., and Ray, A. S., *Mater. Res. Bull*. **33**, 1303 (1998).
27. Mangnus, P. J., Bos, A., and Moulijn, J. A., *J. Catal*. **146**, 437 (1994).
28. Scheffer, B., Mangnus, P. J., and Moulijn, J. A., *J. Catal*. **121**, 18 (1990).
29. Bartholomew, C. H., *Appl. Catal. A—Gen*. **212**, 17 (2001).